ELSEVIER

Physica B 246–247 (1998) 549–552

PHYSICA B

Single crystal EPR of Mn_{12}-acetate clusters

S. Hill[a,*], J.A.A.J. Perenboom[b], T. Stalcup[a], N.S. Dalal[c], T. Hathaway[c], J.S. Brooks[a]

[a] *National High Magnetic Field Laboratory, Florida State University, Tallahassee, FL 32310, USA*

[b] *Research Institute for Materials and High Field Magnet Laboratory, University of Nijmegen, NL-6525 ED Nijmegen, The Netherlands*

[c] *Chemistry Department and National High Magnetic Field Laboratory, Florida State University, Tallahassee, FL 32310, USA*

Abstract

We have used electron paramagnetic resonance (EPR) to study the energy level diagram of the Mn_{12}-cluster compound, in the frequency range from 35 to 115 GHz. Our high sensitivity allows the observation of multiple resonances, and their temperature dependence, on high-quality single crystals. The results are in qualitative agreement with the picture of a strong axial anisotropy. Measurements with the field applied parallel and perpendicular to the easy axis reveal significant zero-field splittings and level crossings, as predicted theoretically.

PACS: 75.45. + j; 36.40.Cg; 76.30. − v; 07.57.Pt

Keywords: Electron paramagnetic resonance; Mn_{12}-Acetate

The Mn_{12} cluster complex, $[Mn_{12}O_{12}(CH_3COO)_{16}(H_2O)_4] \cdot 2CH_3COOH \cdot 4H_2O$ (Mn_{12}-Ac), has attracted considerable interest because it is believed to exhibit macroscopic quantum tunneling of magnetic moment (QTM) [1–3]. The core of the cluster consists of a tetrahedron of four Mn(IV) ions, each in their $S = \frac{3}{2}$ state coupled to yield $S = 6$, surrounded by eight Mn(III) ions each with $S = 2$ producing a moment $S = 16$ directed anti-parallel to the spin of the inner ions [4]. In the ground state, the cluster therefore acts as a single $S = 10$ system, with the spin preferentially aligned along the c-axis due to a large axial crystal field anisotropy in the tetragonal lattice.

To lowest order, the Hamiltonian may be written $H_o = -D_1 S_Z^2 - g\mu_B \boldsymbol{B}.\boldsymbol{S}$ [5]. Thus, the $\pm S_Z$ levels are degenerate in zero field, the $S_Z = \pm 10$ levels lying lowest in energy, and the $S_Z = 0$ level lying highest. Fig. 1 shows a portion of the energy level

* Correspondence address. Permanent address: Department of Physics, Montana State University, Bozeman MT 59717, USA. Tel.: + 1 406 994 3614; fax: + 1 406 994 4452; e-mail: hill@physics.montana.edu.

0921-4526/98/$19.00
PII S0921-4526(97)00984-8

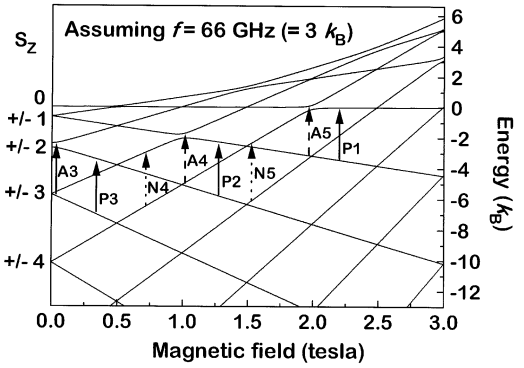

Fig. 1. Energy diagram for the field parallel to the sample's easy axis [6]. See text for explanation of symbols.

diagram obtained by diagonalizing the spin hamiltonian, and using a number of recently obtained experimental input parameters [6,7]. When the system is spin polarized by applying and removing a large magnetic field ($g\mu_B \boldsymbol{B} \gg D_1$) parallel to the sample's easy axis, a considerable energy barrier inhibits the reversal of this moment; the magnitude of this barrier is $\sim 10^2 \times D_1 \approx 64$ K [7]. In spite of this, considerable experimental evidence suggests that the spin system is somehow able to overcome this barrier at low temperatures [1–3].

Below about 3 K, steps are observed in the hysteresis loop of oriented powder samples and single crystals [1–3,6,7]. The occurrence of these steps, at regularly spaced values of magnetic field, is an indication that the magnetization reversal is due to QTM [1]. Unlike superparamagnetic particles, where QTM was first observed [1], Mn_{12}-Ac contains a large number of identical spin clusters, allowing much more accurate comparisons to be made.

Until now, no single crystal EPR studies of Mn_{12}-Ac have been possible. This has been due to the small sizes of typical single crystals, and the low sensitivity of high frequency EPR techniques deemed necessary to probe the energy levels of this system. Nevertheless, high-frequency EPR studies on polycrystalline samples have provided estimates for some parameters in the spin Hamiltonian [8].

In this work we have used lower frequencies (35–115 GHz), in combination with an extremely sensitive cavity perturbation technique, to study single crystals. This frequency interval exceeds the zero-field splittings for the low S_Z states close to the barrier (see Fig. 1); thus, by populating these levels, extremely precise information concerning the spin Hamiltonian may be obtained. Furthermore, recent AC susceptibility measurements indicate that QTM occurs via precisely these low S_Z levels [9].

Slightly oversized cylindrical copper cavities were used in transmission, providing several modes in the desired frequency range [10]; predominantly TE01p ($p = 0, 1, 2 \ldots$) modes were excited, with quality factors of the order of 10^4. A single Mn_{12}-Ac crystal was placed close to the bottom of the cavity, half way between its axis and its perimeter, thereby ensuring that the sample was optimally coupled to the radial AC magnetic fields for a given TE01p mode. The applied DC magnetic field was directed parallel to the cavity axis. The sample was loaded in three configurations, with the DC field applied parallel to each of the sample's a-, b- and c-axis. The sample dimensions were $\sim 1 \times 0.5 \times 0.2\,\mathrm{mm}^3$. The cavity and, therefore, the sample could be maintained at any temperature in the range from 1.25 to 60 K. Both superconducting and Bitter-type magnets were employed. As a source and detector, we utilised a Millimeter-wave vector network analyzer (MVNA) [10]. The vector capability of the MVNA allowed us to directly measure the absorption and dispersion in the cavity. No field modulation is necessary.

Fig. 2 shows normalized transmission through the cavity, at different temperatures, for the field parallel to the sample's easy axis – the frequency is 66.135 GHz. The sharp minima correspond to absorption in the sample due to EPR; complementary data were obtained for the dispersion. A strong feature is observed at 2.5 T (labelled X), which broadens on cooling. From the frequency dependence, we have established that this feature has $g = 2.07 \pm 0.02$ and negligible zero-field offset. Such a feature cannot be reconciled with the energy diagram (see Fig. 1) and is believed to be due to isolated impurities in the sample – no features are observed in the empty cavity.

As the temperature is raised, the EPR spectra in Fig. 2 develop new resonances on the low field side of the impurity resonance. The frequency dependence of these features indicate g-values of

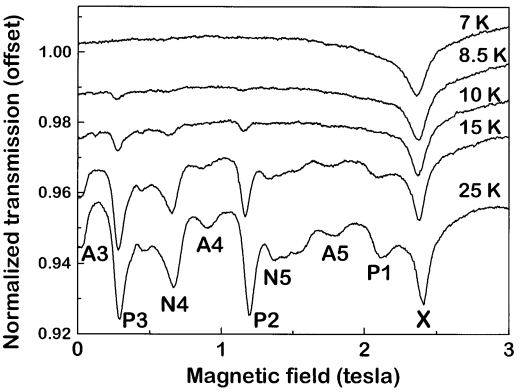

Fig. 2. Temperature dependence of the EPR spectra obtained with the field parallel to the sample's easy axis; the frequency is 66 GHz. See text for explanation of symbols.

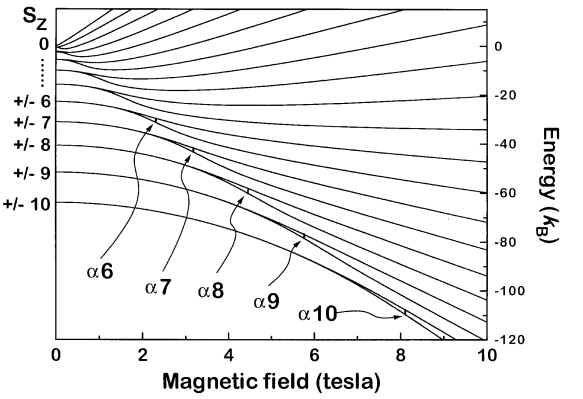

Fig. 3. Energy diagram for the field perpendicular to the sample's easy axis [6]. See text for explanation of symbols.

$+2.1 \pm 0.02$ and -2.1 ± 0.02, with a series of different zero-field offsets. The lowest field features possess the largest zero-field offsets, which are in approximate agreement with zero-field splittings calculated for the low S_Z levels in Fig. 1 [6]. The temperature dependence of the resonance intensities is consistent with the thermal population of these levels.

We have indicated, in Fig. 1, the transitions which we believe correspond to the resonances in Fig. 2. It can be seen from Fig. 1 that, for each pair of zero-field levels ($\pm S_Z$), two series of transitions are observed. The resonances in Fig. 2 have been labelled P ($g = +2.10$) and N ($g = -2.10$) to distinguish between these cases. Additional resonances due to anticrossings, caused by an appreciable fourth-order term in the spin Hamiltonian [6], are also observed and labelled A. The numbering after the letters P, N or A refers to the S_Z value for the level from which the transition was excited.

Although the frequencies used here are smaller than the larger zero-field splittings, we have been able to obtain a considerable amount of information concerning spin states close to the barrier. We suspect, from the observed anticrossings, and from other recent measurements [6], that higher-order terms in the spin Hamiltonian are therefore important; indeed, these were taken into account in the calculation of Fig. 1 [6].

The nature of the energy diagram for the field perpendicular orientation ($\boldsymbol{B} \perp c$) allows us to probe the entire zero-field structure of the system. This can be seen from Fig. 3, where the application of a perpendicular DC field causes a strong mixing and anticrossing of levels separated by $\Delta S_Z = 1$. The result is a lifting of the degeneracy between the $\pm S_Z$ levels and, because of level mixing, the possibility of transitions between these levels.

Fig. 4 shows EPR spectra obtained at several temperatures, for the field perpendicular orientation; the frequency is 44.237 GHz. Most of the resonances can be attributed to transitions between split $\pm S_Z$ levels (labelled α), and are indicated in Fig. 3. The impurity resonance is again observed (labelled X). In contrast to the field parallel orientation, all of the resonances are observed at fields above the impurity feature. Thus, the data in Figs. 2 and 4 confirm the high degree of axial anisotropy. Measurements for the field parallel to the *a*- and *b*-axis rule out any orthorhombic distortions of the crystal symmetry down to ~ 5 K. The temperature dependence in Fig. 4, together with the relative intensities of the principal resonances (labelled α), is expected qualitatively assuming a thermal population of the higher lying spin states. However, there are some additional features in Fig. 4 (labelled β) which remain difficult to reconcile with the energy diagram. These features may be due to twinning in the crystal, though this is

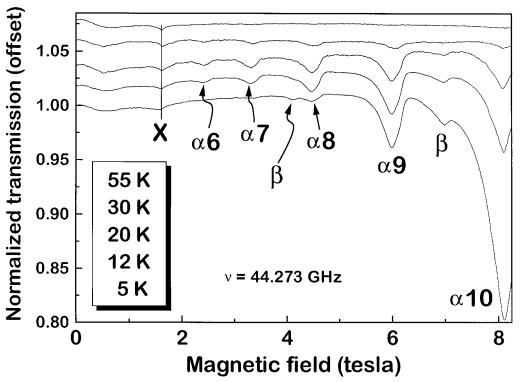

Fig. 4. EPR spectra obtained with the field perpendicular to the sample's easy axis. The temperatures in the inset correspond, from top to bottom, to the temperatures at which data in the main part of the figure were taken. See text for explanation of symbols.

unlikely given the similarity of spectra obtained for the field parallel to the *a*- and *b*-axis.

In conclusion, we have performed single crystal EPR measurements on the Mn_{12}-Ac compound. Although the frequencies used in this study are lower than those used in previous studies [8], we have been able to obtain a considerable amount of information concerning spin states close to the barrier. Our findings are in reasonable agreement with recent models and further work is in progress.

This work was supported under NSF-DMR 95-10427 and by the National High Magnetic Field Laboratory.

Note added in proof. We have recently become aware of a related EPR study by Barra et al., Phys. Rev. B, in press.

References

[1] For a review, see Quantum Tunneling of Magnetization – QTM'94, L. Gunther, B. Barbara (Eds.), vol. 301 of NATO ASI Series E: Applied Sciences, Kluwer, Dordrecht, 1995.
[2] J.R. Frideman, M.P. Sarachik, J. Tejada, R. Ziolo, Phys. Rev. Lett. 76 (1996) 3830.
[3] L. Thomas, F. Lionti, R. Ballou, D. Gatteschi, R. Sessoli, B. Barbara, Nature 383 (1996) 145.
[4] R. Sessoli, H.-L. Tsai, A.R. Scake, S. Wang, J.B. Vincent, K. Folting, D. Gatteschi, G. Christou, D.N. Hendrickson, J. Am. Chem. Soc. 115 (1993) 1804.
[5] P. Politi, A. Rettori, F. Hartmann-Boutron, J. Villain, Phys. Rev. Lett. 75 (1995) 537.
[6] J.A.A.J. Perenboom et al., in these Proceedings (RHMF '97), Physica B 246–247 (1998).
[7] M.A. Novak, R. Sessoli, A. Caneschi, D. Gatteschi, J. Magn. Magn. Mat. 146 (1995) 211.
[8] A. Caneschi, D. Gatteschi, R. Sessoli, A.L. Barra, L.-C. Brunel, M. Guillot, J. Am. Chem. Soc. 113 (1991) 5873.
[9] F. Luis, J. Bartolome, J.F. Fernandez, J. Tejada, J.M. Hernandez, X.X. Zhang, R. Ziolo, Phys. Rev. B 55 (1997) 11448.
[10] S. Hill, P.S. Sandhu, C. Buhler, S. Uji, J.S. Brooks, L. Seger, M. Boonman, A. Wittlin, J.A.A.J. Perenboom, P. Goy, R. Kato, H. Sawa, S. Aonuma, in: Mohammed N. Afsar (Ed.), Millimeter and Submillimeter Waves III, Proc. SPIE, vol. 2842, 1996, p. 296.